Vietnam Journal of Science and Technology ***64***(1) (2026) 162–174
DOI: https://doi.org/10.15625/2525-2518/20799

Novel distributed control for multi-agent systems: Application to a quadcopter formation

M. Xuan Nguyen*

Faculty of Engineering, Dong Nai Technology University, Bien Hoa, Dong Nai, Viet Nam

*Email: *nguyen_xuan@dntu.edu.vn*

Received: 15 June 2024; Accepted for publication: 15 October 2024

Abstract. Multi-agent systems (MAS) are well-known for overweighting single agents that exhibit several complex tasks. This paper introduces a novel approach to modeling and controlling a multi-agent system (MAS) employing a directed and switchable topology. The dynamics of the MAS are represented using a mass-spring system model, in which each agent is treated as a mass, and the inter-agent relative positions act as springs, generating formation forces. The concept of a "formation equilibrium point" is introduced to characterize the formation's condition in terms of formation force. By analyzing these equilibria, a formation control law is derived to ensure the achievement of the desired formation pattern and shape. It is worth highlighting that the formation controller is implemented in each agent, so the MAS does not require a powerful computer, which serves as a cntral formation control station. Illustrative examples are conducted with a quadcopter formation. The effectiveness of the proposed algorithm is demonstrated through various numerical simulations.

Keywords: distributed control, multi-agent system, formation control, quadcopter.

Classification numbers: 5.3.7, 5.8, 5.10.2.

1. INTRODUCTION

In recent years, the multi-agent system control and its applications to quadcopter formation flight have attracted significant worldwide attention [1-4]. Quadcopters offer advantages such as rapid maneuverability, a simple structure, high reliability, and cost-effectiveness compared to other unmanned aerial vehicles (UAVs). As a result, their applications can be seen in diverse areas, including environmental exploration, atmospheric studies, disaster monitoring, search and rescue operations, surveillance, risk zone inspections, and aerial mapping. The collective flight of multiple quadcopters, as opposed to individual ones, presents numerous benefits, such as increased payload capacity, expanded sensor capabilities, broader surveillance coverage, and the ability to accomplish complex tasks [5]. However, addressing the formation control problem requires complex analyses encompassing system modeling, control design, and inter-communication.

Various strategies have been proposed for the formation control of multiple quadcopters. Some studies, such as those in [6, 7], introduced leader-follower formation control algorithms. However, these approaches were limited to resolving formation control in two-dimensional

space (X-Y plane) and did not consider relative positions during formation shape-keeping tasks. Other methods, like in [8], focused on flock formation control but solely addressed shape-keeping without mentioning formation pattern-achieving. References [9-14] tackled formation control using consensus approaches with either undirected or fixed intercommunication topologies, which proved resource-intensive and non-scalable.

To address these drawbacks, studies have emerged on formation control with directed and switching interaction topologies. Reference [15] proposed a method with directed and switching topologies for UAVs to achieve consensus motions, while [16] presented an algorithm for second-order multi-agent systems' formation control. Despite these efforts, challenges persist, with limited research capable of providing a formation control algorithm accommodating both directed and switching topologies. The references above underscore the ongoing challenge faced by worldwide researchers in achieving formation control for multiple UAVs. Most of the prior research on formation control for multi-agent systems has been limited to either undirected or fixed topologies, with only a few able to offer an algorithm incorporating both directed and switching topologies.

In response to these observations, we conducted an examination of the formation structure and formation control law governing multiple quadrotor systems. This paper introduces a novel modeling and control design method inspired by the conventional mass-spring system, defining formation spring and force terms to represent the connections between agents. Each agent is treated as a rigid mass connected to other agents through formation springs, forming a linear state-space model for the entire formation. A formation equilibrium state controller is proposed using an integral linear quadratic regulator (LQR) optimal control method. The overall control scheme includes high-level and low-level controllers, with a distributed algorithm in the high-level controller for generating reference positions and PID controllers in the low-level controller for position tracking.

Compared with the related existing works, the contributions of this approach are as follows. First, the use of a mass-spring system model offers a straightforward and visual method for formation modeling and control, with simple stability and controllability analyses. Second, this study considers directed and switching inter-communication topologies. In addition, distributed formation control laws are proposed based on the formation dynamics model, conserving computation resources and ensuring fast convergence. Finally, numerical simulations validate the effectiveness of the proposed method.

2. PROBLEM STATEMENT AND PRELIMINARIES

2.1. Two-mass – one-spring system

Consider a viscous friction-free mechanical system, as in Figure 1. The system consists of two masses, namely m_1 and m_2, connecting to each other via a spring with a stiffness of k.

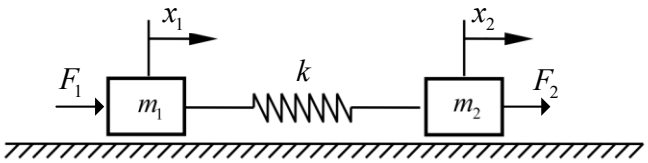

Figure 1. A two-mass – one-spring system consists of two masses connecting via a spring.

Let vector $x=[x_1,x_2]^T \in \mathbb{R}^2$ represents the displacement of m_1, m_2 from a predefined origin, and vector $F=[F_1, F_2]^T \in \mathbb{R}^2$ denotes external forces applied to each mass (see Figure 1). Thus, we have:

$$\begin{bmatrix} m_1 & 0 \\ 0 & m_2 \end{bmatrix}\begin{bmatrix} \ddot{x}_1 \\ \ddot{x}_2 \end{bmatrix}+\begin{bmatrix} k & -k \\ -k & k \end{bmatrix}\begin{bmatrix} x_1 \\ x_2 \end{bmatrix}=\begin{bmatrix} F_1 \\ F_2 \end{bmatrix} \tag{1}$$

Manipulating (1), one can get:

$$\ddot{x}_2-\ddot{x}_1+\frac{k(m_1+m_2)}{m_1m_2}(x_2-x_1)=\frac{F_2}{m_2}-\frac{F_1}{m_1} \tag{2}$$

Let us define the following state variable, representing the relative position and velocity between the masses.

$$\xi=\begin{bmatrix} x_2-x_1 \\ \dot{x}_2-\dot{x}_1 \end{bmatrix} \tag{3}$$

Then, Eq. (2) can be reformulated in the form of a state-space model as:

$$\begin{cases} \dot{\xi}=A\xi+Bu \\ \zeta=C\xi \end{cases} \tag{4}$$

where

$$A=\begin{bmatrix} 0 & 1 \\ -\dfrac{k(m_1+m_2)}{m_1m_2} & 0 \end{bmatrix},\ B=\begin{bmatrix} 0 \\ 1 \end{bmatrix},\ C=\begin{bmatrix} 1 & 0 \\ 0 & 1 \end{bmatrix},\ u=\frac{F_2}{m_2}-\frac{F_1}{m_1} \tag{5}$$

2.2. Quadcopter dynamics

Let ϕ, θ, and ψ respectively represent the roll, pitch, and yaw angles ($|\phi|<\pi/2$ and $|\theta|<\pi/2$); x, y, and z denote the quadcopter's position along the inertial x, y, and z axes (Figure 2). Let I_x, I_y, and I_z be the inertia momentums along the x, y, and z axes, respectively, in the body-fixed frame, m the mass, and l_a the arm length of vehicle; $u=[u_T, u_p, u_q, u_r]^T$ is the control input, and g is the gravitational acceleration. Then, the quadcopter dynamics can be described as follows [17]:

$$\begin{cases} \dot{p} = \left(\dfrac{I_y - I_z}{I_x} \right) qr + \dfrac{1}{I_x} u_p \\ \dot{q} = \left(\dfrac{I_z - I_x}{I_y} \right) rp + \dfrac{1}{I_y} u_q \\ \dot{r} = \left(\dfrac{I_x - I_y}{I_z} \right) pq + \dfrac{1}{I_z} u_r \\ \ddot{x} = \dfrac{1}{m} \left(\cos\phi \sin\theta \cos\psi + \sin\phi \sin\psi \right) u_T \\ \ddot{y} = \dfrac{1}{m} \left(\cos\phi \sin\theta \sin\psi - \sin\phi \cos\psi \right) u_T \\ \ddot{z} = g - \dfrac{1}{m} \left(\cos\phi \cos\theta \right) u_T \end{cases} \tag{6}$$

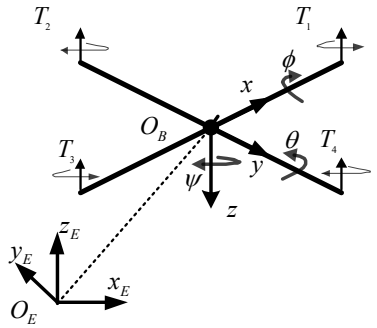

Figure 2. The quadcopter consists of four motors, out of which two motors (1 and 3) rotate counterclockwise, and the other two (2 and 4) rotate clockwise.

The control input u is computed from the motor's forces, $T_i = c_T \Omega_i^2, (i = 1,2,3,4)$, as follows

$$\begin{cases} u_T = T_1 + T_2 + T_3 + T_4 \\ u_p = l_a (T_2 - T_4) \\ u_q = l_a (T_1 - T_3) \\ u_r = c_D \left(T_1 + T_3 - T_2 - T_4 \right) \end{cases} \tag{7}$$

where, Ω_i is the i th-motor's speed; c_T and c_D are the thrust and drag coefficients.

2.3. Preliminaries

Assumption 1 *(inter-communication topology):* All quadcopters have a bidirectional connection to each other (quadcopters have access to the information of one another).

Notation 1: Consider a multi-agent quadcopter system. Let n denote the number of quadcopters. Set $\Upsilon = \{1,...,n\}$. $i \in \Upsilon$. M_i represents ith quadcopter. The leader is denoted by M_1. The formation force caused by the spring between agent M_i and agent M_j (briefly called formation force between M_i and M_j) is denoted by F_{ji} or F_{ij} ($F_{ij} = -F_{ji}$ and $F_{ii} = 0$). The symbol $\sum F^{(i)}$ represents

total formation force acting on M_i, F_i is a control input (force) applied to control M_i. A vector $\rho_i = (x_i, y_i, z_i)$ and a vector $\Theta_i = (\phi_i, \theta_i, \psi_i)$ respectively represent the position and attitude of M_i.

2.4. Control objective

The control scheme of each agent involves two loops, i.e., high-level and low-level controllers. While the high-level loop plays the role of generating referenced trajectory ρ_d, the low-level loop guarantees that the vehicle tracks the references. The integration of the two loops is to force the formation error to zero, i.e., $\lim_{t\to\infty}(\rho - \rho_d) = 0$. The main results of this work focus on finding a novel high-level control law, which will be called formation controller hereafter.

3. MAIN RESULTS

3.1. Mass-spring system-based MAS's dynamics model

In order to utilize the mass-spring system concept for the dynamic modelling of a MAS, the following definitions are introduced.

Definition 1 *(formation spring):* Invisible connection between the positions of each two agents in a formation is called a formation spring. Each terminal of the formation spring is attached to one agent (Figure 3). Stiffness of a formation spring is denoted by K_f and represents the intensity of connection. The unit of the formation spring's stiffness is N/m.

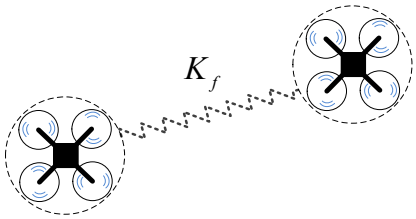

Figure 3. A formation spring is defined to describe the connection between the positions of two agents.

Definition 2 *(formation force):* A force vector induced by a formation spring is called a formation force, F_f, with the following properties.

The direction of F_f is colinear with the direction of the formation spring.

The magnitude of F_f is proportional to the extension/compression, Δl, of the formation spring.

$$F_f = -K_f \Delta l \tag{8}$$

Definition 3 *(formation equilibrium state of an agent):* The state of an agent at which the vector sum of all formation forces acting on the agent is zero is called the formation equilibrium state of the agent.

$$\sum F_f = 0 \tag{9}$$

Definition 2 indicates that the formation forces are independent of the mass of the agents. Thus, for the sake of simplicity, all mass of the agents are set as *m,* and all formation spring's stiffness are set as K_f .

$$\begin{bmatrix} m & 0 & \cdots & 0 \\ 0 & m & \cdots & 0 \\ \vdots & \vdots & \ddots & \vdots \\ 0 & 0 & \cdots & m \end{bmatrix} \begin{bmatrix} \ddot{\rho}_1 \\ \ddot{\rho}_2 \\ \vdots \\ \ddot{\rho}_n \end{bmatrix} + \begin{bmatrix} (n-1)K_f & -K_f & \cdots & -K_f \\ -K_f & (n-1)K_f & \cdots & -K_f \\ \vdots & \vdots & \ddots & \vdots \\ -K_f & -K_f & \cdots & (n-1)K_f \end{bmatrix} \begin{bmatrix} \rho_1 \\ \rho_2 \\ \vdots \\ \rho_n \end{bmatrix} = \begin{bmatrix} F_1 \\ F_2 \\ \vdots \\ F_n \end{bmatrix} \tag{10}$$

In (10), subtracting the *i*-th row by the first-row yields:

$$m(\ddot{\rho}_i - \ddot{\rho}_1) + n_i K_f (\rho_i - \rho_1) = F_i - F_1 \tag{11}$$

Let

$$\xi_i = \begin{bmatrix} \rho_i - \rho_1 \\ \dot{\rho}_i - \dot{\rho}_1 \end{bmatrix} \tag{12}$$

Then

$$\begin{cases} \dot{\xi}_i = A_i \xi_i + B_i u_i \\ \zeta_{i1} = C_i \xi_i \end{cases} \tag{13}$$

where

$$A_i = \begin{bmatrix} 0 & 1 \\ -\dfrac{n_i K_f}{m} & 0 \end{bmatrix}, B_i = \begin{bmatrix} 0 \\ 1 \end{bmatrix}, C_i = \begin{bmatrix} 1 & 0 \\ 0 & 1 \end{bmatrix}, u_i = \frac{1}{m}(F_i - F_1) \tag{14}$$

3.2. Formation controller

The formation controller, presented in this subsection, consists of two parts, i.e., the reference generator and the formation equilibrium state controller.

3.2.1. Reference generator

We are now moving on to designing the reference generator.

The formation force between agents M_i and M_j acting on the agent M_i is as:

$$F_{ji} = -K_f (x_i - x_j) \tag{15}$$

When Assumption 1 is satisfied, the sum of all formation forces acting on agent M_i is:

$$\sum F^{(i)} = F_i - K_f \sum_{j=1}^{n} (x_i - x_j) \tag{16}$$

The formation force acting on M_1 is desired to be zero throughout the flight.

$$\sum F^{(1)} = F_1 - K_f \sum_{l=2}^{n} (x_1 - x_l) = 0 \tag{17}$$

or

$$F_1 = K_f \sum_{l=2}^{n} (x_1 - x_l) \tag{18}$$

From (14), we have:

$$F_i = mu_i + F_1 \tag{19}$$

From (16), (18), and (19), the following are obtained:

$$\begin{aligned} \sum F^{(i)} &= mu_i + K_f \sum_{l=2}^{n} (x_1 - x_l) - K_f \sum_{j=1}^{n} (x_i - x_j) \\ &= mu_i - K_f \left[\sum_{l=2}^{n} x_l - (n-1)x_1 \right] - K_f \left[nx_i - x_1 - \sum_{j=2}^{n} x_j \right] \\ &= mu_i - nK_f (x_i - x_1) \end{aligned} \tag{20}$$

This total force $\sum F^{(i)}$ drives M_i toward the position x_{di} which satisfies:

$$\sum F^{(i)} = K_f \sum_{j=1}^{n} (x_{di} - x_j) \tag{21}$$

which can be rewritten as:

$$mu_i - nK_f (x_i - x_1) = K_f \sum_{\substack{j=1 \\ j \neq i}}^{n} (x_{di} - x_j) = K_f \left[(n-1)x_{di} - x_1 - \sum_{\substack{j=2 \\ j \neq i}}^{n} x_j \right] \tag{23}$$

Manipulating (22), we obtain:

$$x_{di} = \frac{m}{(n-1)K_f} u_i - \frac{1}{n-1} \left[nx_i - \sum_{\substack{j=2 \\ j \neq i}}^{n} x_j - (n+1)x_1 \right] \tag{24}$$

Remark 3: The proposed algorithm is considered a distributed controller as it is implemented in each agent, and it generates the trajectory reference for the agent by using that agent's feedback information and the relative state of that agent in relation to other agents.

3.2.2. Formation equilibrium state controller

The controllability of the system in (13) is analyzed through a controllability matrix, C_m, which is defined as:

$$C_m = [B_i \quad A_i B_i] = \begin{bmatrix} 0 & 1 \\ 1 & 0 \end{bmatrix} \tag{25}$$

It is straightforward to say that C_m is a full rank matrix. Therefore, it is concluded that the system (13) is controllable.

The full control scheme of each quadcopter consists of a two-level controller, namely the high-and low-level controllers, as shown in Figure 4.

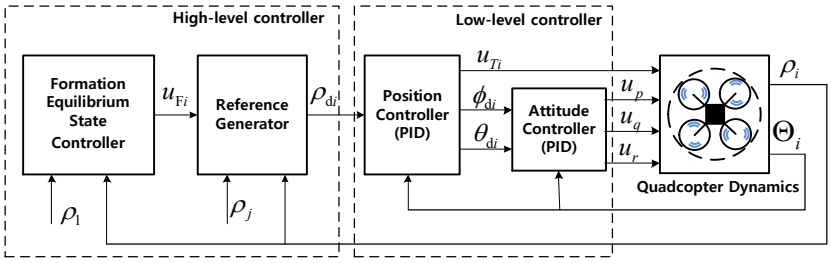

Figure 4. The distributed control scheme is implemented on each agent in the high-level controller.

The formation equilibrium state controller is designed as an integral linear quadratic regulator (LQR) controller:

$$u_{Fi} = -\gamma \xi_i + \gamma_I \int_0^t e_\zeta \, \mathrm{d}\tau \tag{26}$$

where, $e_\zeta = \zeta_{i1d} - \zeta_{i1}$. γ and γ_I are controller gains.

The control laws in (25) can be described by a block diagram, as shown in Figure 5.

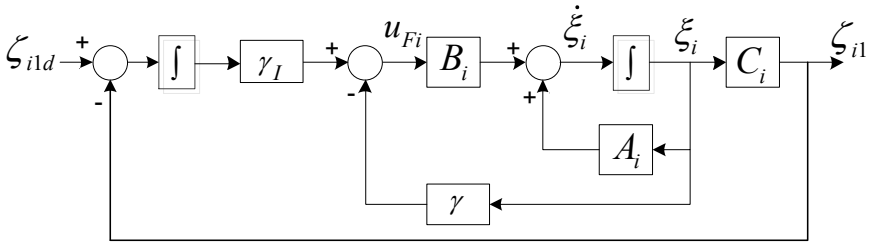

Figure 5. Block diagram of the formation equilibrium state controller.

Remark 1: Clearly, $\zeta_{ij} \to \zeta_{ij\mathrm{d}}$ as $\zeta_{i1} \to \zeta_{i1\mathrm{d}}$ and $\zeta_{j1} \to \zeta_{j1\mathrm{d}}$.

Remark 2: The integral term in the control law (25) plays the role of removing steady-state errors (if any) existing in the control performance.

4. SIMULATION RESULTS AND DISCUSSIONS

4.1. Simulation assumptions

The simulation is conducted based on the following assumptions: (i) the attitude information of each agent is determined by an inertial navigation system (INS), (ii) the agent's

altitude is measured either by a ranging sensor, and (iii) the agent's horizontal position is provided by a global positioning system (GPS) receiver module. The agent's dynamical parameters used for the simulation are shown in Table 1.

In order to effectively demonstrate the proposed method's efficacy, the simulation of formation flight control involved two stages corresponding to switching topologies, namely Topo. 1 and Topo. 2, as illustrated in Figure 6. Each green arrow within Figure 6 represents inter-communication between two agents. For instance, in Topo. 1, quadcopter M_2 directly accesses information from the virtual leader M_1, while M_3 only has access to information from M_2, and so forth. Meanwhile, Topo. 2 is configured in a reverse manner, presenting an alternative arrangement of inter-communication dynamics.

The trajectory of the virtual leader is predefined as: $(x^d, y^d, z^d) = (0.3t, 0.3t, 0.3t)$. The formation pattern is planned through the desired relative distances between the quadcopters as: $\zeta_{21}^d = [0,1,0]^T$, $\zeta_{32}^d = [-1,-2,0]^T$, $\zeta_{43}^d = [2,0,0]^T$, and $\zeta_{14}^d = [-1,1,0]^T$. The initial states, including position and velocity, of the quadcopters are listed in Table 2.

Table 1. Quadcopter's dynamic parameters used for simulation.

Symbol	Value and unit
m	1.80 kg
I_x	0.0121 kg.m^2
I_y	0.0119 kg.m^2
I_z	0.0223 kg.m^2
l_a	0.23 m
g	9.81 m/s^2

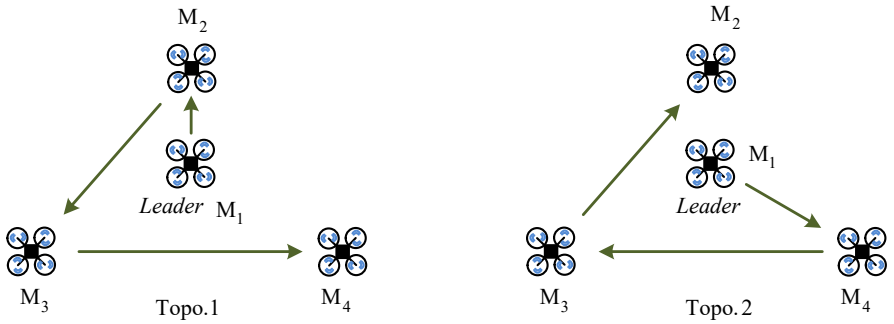

Figure 6. Two inter-communication topologies (Topo. 1 and Topo. 2) are used in the simulation. The agents are desired to form a triangle formation pattern with the leader at the center and the others at the corners.

Table 2. Initial positions of the agents.

Symbol	Value and unit
$p_1(0)$	$[0,0,0]^T$
$p_2(0)$	$[-0.5,1.5,0]^T$
$p_3(0)$	$[-1.5,-1.5,0]^T$
$p_4(0)$	$[1.5,-1.2,0]^T$

4.2. Simulation results

The initial stage of the simulation (Stage 1) spans from $t = 0$ to $t = 50$ s. At the onset, the vehicles are initialized and commence movement from their initial positions. Guided by the proposed controller, the agents follow the trajectory reference within a few seconds, as depicted in Figures 7 and 8. The convergence time remains consistent at around 7 s for all agents. Nevertheless, owing to the predefined inter-communication topology, the agents exhibit varying amplitudes of oscillation in their position control performance, as illustrated in Figure 8(a). Specifically, for agent M_2, the oscillations are 0.1 m, 0.12 m, and 0.11 m along the x-, y-, and z-axis, respectively. Agent M_3 exhibits oscillations of 0.15 m, 0.08 m, and 0.21 m for the x-, y-, and z-position, respectively. Concurrently, agent M_4 experiences oscillations of 0.3 m, 0.06 m, and 0.27 m for its x-, y-, and z-positions. The velocities of the agents also stabilize at the desired values after a short period of oscillation, as shown in Figure 8(b). This rapid convergence enables the agents to promptly achieve the formation pattern and adhere to the desired trajectory.

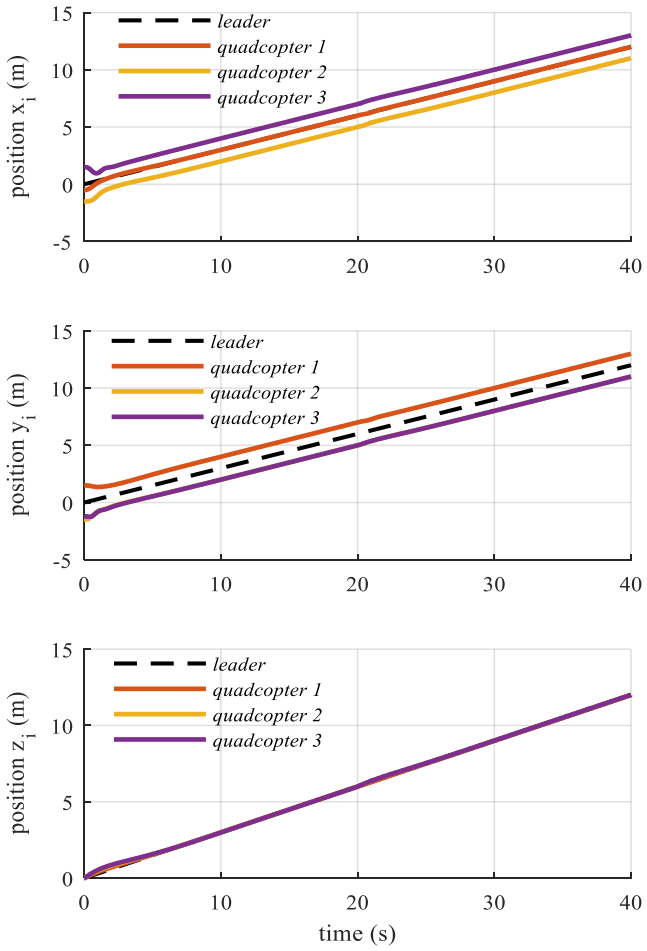

Figure 7. Formation pattern achieving and formation trajectory tracking control performance of the agents along the x-, y-, and z-axis.

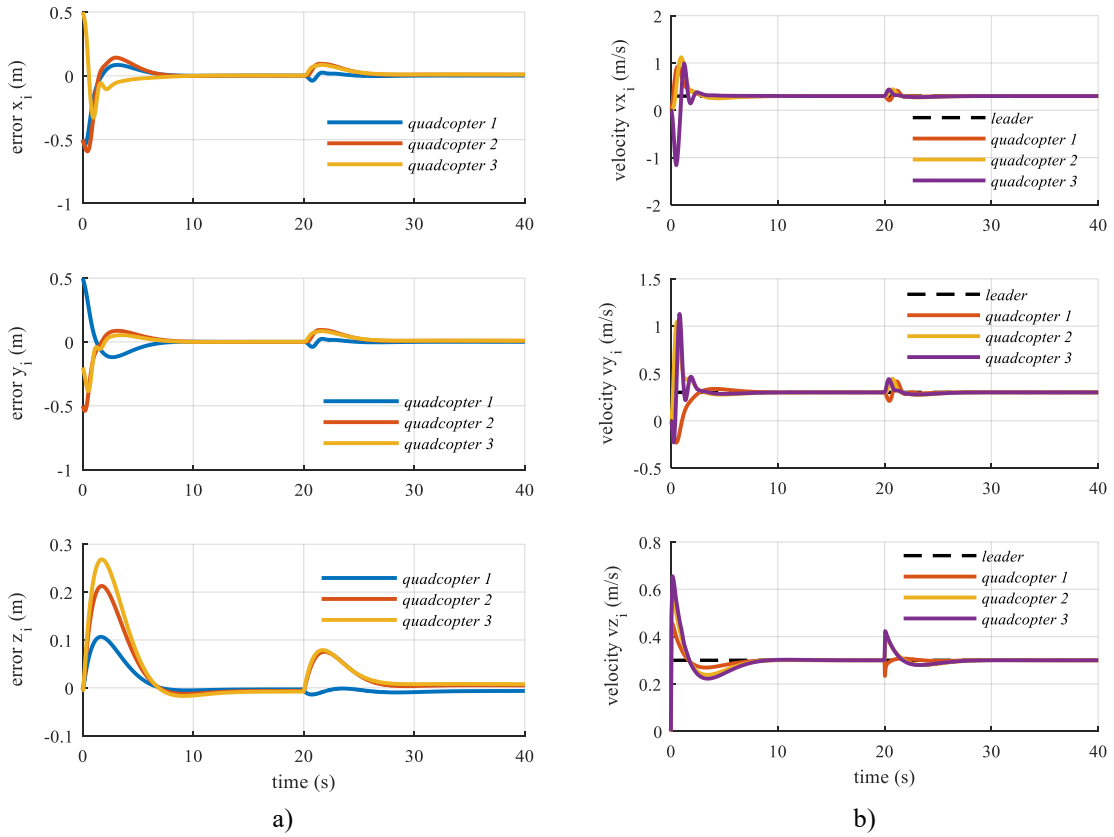

Figure 8. (a) Position tracking error performance of the agents along the x-, y-, and z-axis; and (b) Velocity performance of the agents along the x-, y-, and z-axis.

At $t = 20$ s, the beginning of the second stage (Stage 2), a sudden switch in the inter-communication topology from Topo. 1 to Topo. 2 is triggered. Consequently, the formation control performance experiences inevitable oscillations. As depicted in Figure 8, the position control performance of the agents demonstrates peak-to-peak amplitudes of oscillation not exceeding 0.1 m for x-, y-, and z-positions. The formation pattern rapidly re-establishes, and the formation trajectory remains stable after approximately 6 seconds. In real-world applications, such circumstances may arise due to intentional human actions or, sometimes, accidents resulting from system faults. The rapid response of our proposed method holds the potential for a variety of reliable and efficient formation flight applications that exert switching inter-communication topologies to achieve complex tasks.

5. CONCLUSIONS

This work introduced a novel strategy to address the distributed control problem of a MAS. Based on the mass-spring system, the formation dynamic model is obtained and used in the design of the formation controller. The proposed algorithm is applied to a quadcopter formation flight control with a time-varying inter-communication topology. The simulation results illustrate the efficacy of our approach in attaining the desired formation, accurately following the formation trajectory, and sustaining the formation shape during topology changes.

Nonetheless, it's worth noting that the formation was represented using a mass-spring model, overlooking disturbances affecting inter-communication. Exploring a robust adaptive formation control algorithm to handle perturbations stands out as a compelling future work.

CRediT authorship contribution statement. M. Xuan Nguyen: Conceptualization, Methodology, Investigation, Funding acquisition, Software, Writing – original draft, Writing – review & editing, Supervision.

Declaration of competing interest. The authors declare that they have no known competing financial interests or personal relationships that could have appeared to influence the work reported in this paper.

REFERENCES

1. Idrissi M., Salami M., Annaz F. - A review of quadrotor unmanned aerial vehicles: Applications architectural design and control algorithms. J. Intell. Robot. Syst., **104**(2) (2022) 1-33. https://doi.org/10.1007/s10846-021-01527-7.
2. Lee J. W., Xuan-Mung N., Nguyen N. P., Hong S. K. - Adaptive altitude flight control of quadcopter under the ground effect and time-varying load: theory and experiments. J. Vib. Control, **29**(3-4) (2023) 571-581. https://doi.org/10.1177/10775463211050169.
3. Chamola V., Kotesh P., Agarwal A., Naren, Gupta N., Guizani M. - A comprehensive review of unmanned aerial vehicle attacks and neutralization techniques. Ad Hoc Netw., **111** (2021) https://doi.org/10.1016/j.adhoc.2020.102324.
4. Do T. D., Xuan-Mung N., Lee Y. S., Hong S. K. - 2023 9th International Conference on Control, Decision and Information Technologies (CoDIT), (2023) 2151-2157. https://doi.org/10.1109/CoDIT58514.2023.10284286.
5. Abbas R., Wu Q. - Tracking Formation Control for Multiple Quadcopters Based on Fuzzy Logic Controller and Least Square Oriented by Genetic Algorithm. Open Autom. Control Syst. J., **7** (2015) 842-850. https://doi.org/10.2174/1874444301507010842.
6. Abbas R., Wu Q. - Improved Leader-Follower Formation controller for multiple Quadcopters based AFSA. TELKOMNIKA (Telecommunication, Computing, Electronics and Control), **13**(1) (2015) 85-92. https://doi.org/10.12928/telkomnika.v13i1.994.
7. Abas M. F. B., Ali S. A. M., Iwakura D., Song Y., Nonami K. - MAV Circular Leader-Follower Formation Control Utilizing Mass-Spring-Damper with Centripetal Force Consideration. J. Robot. Mechatron., **25** (2013) 240-251. https://doi.org/10.20965/jrm.2013.p0240.
8. Xue R., Song J., Cai G. - Distributed formation flight control of multi-UAV system with nonuniform time-delays and jointly connected topologies. Proc. Inst. Mech. Eng. G: J. Aerosp. Eng., **230**(10) (2016) 1871-1881. https://doi.org/10.1177/0954410015619446.
9. Dong X., Yu B., Shi Z., Zhong Y. - Time-Varying Formation Control for Unmanned Aerial Vehicles: Theories and Applications. IEEE Trans. Control Syst. Technol., **23** (2015) https://doi.org/10.1109/TCST.2014.2314460.
10. Dong X., Zhou Y., Ren Z., Zhong Y. - Time-varying formation control for unmanned aerial vehicles with switching interaction topologies. Control Eng. Pract., **46** (2016) 26-36. https://doi.org/10.1016/j.conengprac.2015.10.001.
11. Abbas R., Wu Q. H. - Adaptive leader follower control for multiple quadcopters via multiple surfaces control. J. Beijing Inst. Technol., **25** (2016)
12. Du H., Zhu W., Wen G., Duan Z., Lü J. - Distributed Formation Control of Multiple Quadcopter Aircraft Based on Nonsmooth Consensus Algorithms. IEEE Trans. Cybern., **49** (2017) 342-353. https://doi.org/10.1109/TCYB.2017.2777463.

13. Zhou Z., Wang H., Hu Z. - Event-Based Time Varying Formation Control for Multiple Quadcopter UAVs with Markovian Switching Topologies. Complexity, **2018**(8124861) (2018) https://doi.org/10.1155/2018/8124861.
14. Qi Y., Zhou S., Kang Y., Yan S. - Formation Control for Unmanned Aerial Vehicles with Directed and Switching Topologies. Int. J. Aerosp. Eng., **2016**(7657452) (2016) https://doi.org/10.1155/2016/7657452.
15. Li Y., Dong X., Li Q., Ren Z. - Proceedings of the 36th Chinese Control Conference, (2017)
16. Xuan-Mung N., Hong S. K. - Improved Altitude Control Algorithm for Quadcopter Unmanned Aerial Vehicles. Appl. Sci., **9**(10) (2019) 2122. https://doi.org/10.3390/app9102122.
17. Ganji S. S., Barari A., Ganji D. D. - Approximate analysis of two-mass-spring systems and buckling of a column. Comput. Math. Appl., **61** (2011) 1088-1095. https://doi.org/10.1016/j.camwa.2010.12.059.